NJC

Accepted Manuscript

This article can be cited before page numbers have been issued, to do this please use: Y. Ban, R. Wang, Y. Li, Z. An, M. Yu, C. Fang, L. Wei and Z. Li, *New J. Chem.*, 2017, DOI: 10.1039/C7NJ04212D.

ROYAL SOCIETY OF CHEMISTRY

rsc.li/njc

View Article Online
DOI: 10.1039/C7NJ04212D

NJC

ARTICLE

Mitochondria-targeted ratiometric fluorescent detection of hydrazine with fast response time

Received 00th January 20xx,
Accepted 00th January 20xx

DOI: 10.1039/x0xx00000x

www.rsc.org/

Yanan Ban,[a//] Ruihui Wang,[b//] Yang Li,[a] Zhen An,[a] Mingming Yu,[a]* Chenjie Fang,[b]* Liuhe Wei[a] and Zhanxian Li[a]

A ratiometric fluorescent probe **1** was synthesized, which exhibited high sensitivity and excellent selectivity in hydrazine recognition. Probe **1** can quantitatively detect hydrazine in concentration range from 30 to 180 μM with the LOD of 2.1 μM. Further, it displayed excellent selectivity, anti-interference over many nucleophilic species, biological species, metal ions and anions, and fast response time (4 min). Due to its ability to target mitochondria, the response of hydrazine to this probe in a living cell was successfully tracked in a ratiometric manner via fluorescence imaging.

Introduction

Hydrazine is not only a highly reactive base and reducing agent, but also a high-energy fuel for rocket-propulsion systems and missile systems.[1] As a result, it plays an important role in many fields such as the pharmaceutical, chemical and agricultural industries.[2–4] On the other hand, as a class of highly toxic and pollutant compound, hydrazine can potentially lead to serious environmental contamination during its manufacture, use, transport and disposal. In addition, as a neurotoxin, hydrazine has several mutagenic effects, which can cause damage to the human health.[5–9] Therefore, it is urgently demanded to develop an efficient and simple method for determining hydrazine level in both environmental and biological science.

Up to now, in order to measure hydrazine, some methods including chromatography-mass spectrometry,[10–12] titration[13] and electrochemical methods[14–18] have been reported, however their shortcomings such as complicated equipment, sample handling and professional operating will limit their application. Therefore, it is still needed to expand new methods which can detect trace hydrazine in situ, with short time and low cost in room temperature.

Fluorescence-based method has been widely used to detect various analytes such as metal ions, anions and biomolecules due to its simplicity, high sensitivity, rapid response, and capacity of real-time and in situ monitoring of the dynamic biological processes in living cells.[19–29] However, available fluorescent probes for hydrazine are still very limited and most of them are turn-on types.[30–36]

Compared with turn-on or turn-off mode fluorescent probes, ratiometric fluorescent probes have many advantages, for example, they can eliminate many interference factors such as optical path length and the illumination intensity. Moreover, when ratiometric fluorescent probes are applied in biosystem, they can realize more effective detection through measuring the ratio of fluorescence intensities at two different wavelengths.[37–40] It is a pity that very few ratiometric fluorescent hydrazine-probe**s** have been reported,[41–47] and it is essential to develop ratiometric fluorescent probes toward hydrazine.

In this paper, using hydrazine-induced fracture of C=C, a highly sensitive, photo-stable ratiometric fluorescent probe **1** (**Scheme 1**) was developed, and the application of which for selective detection and imaging of hydrazine in living cells was successfully demonstrated. The probe exhibited a high sensitivity (the LOD is 2.1 μM), a wide linear response range from hydrazine concentration of 30 to 180 μM, excellent selectivity and anti-interference against other various species, and fast response time. The intrinsic ability of probe **1** to target mitochondrion was confirmed with a co-localization study.

The synthesis of the smart probe **1** was accomplished in 4 steps as shown in **Scheme 1**. The starting materials 2-methyl-8-hydroxyquinoline and acryloyl chloride were reacted for 12 hours under 20°C to give compound 4 in a yield of 47.3%. The product 4 was oxidized by SeO_2 at 101°C to give product **3** in a yield of 71.6%. The reaction of 1,1,2-trimethylbenzo[e]indolenine and CH_3I gave compound **2** in a yield of 52.6%. Probe **1** was obtained in a yield of 45.1% by the Knoevenagel condensation reaction of compound **3** with compound **2**. The detailed synthetic procedures and characterization data are presented in the Experimental section **(**Supporting Information).

[a] *College of Chemistry and Molecular Engineering, Zhengzhou University, Zhengzhou 450001, China. E-mail: yumm@zzu.edu.cn*
[b] *School of Pharmaceutical Sciences, Capital Medical University, Beijing, 100069, China. E-mail: cjfang@ccmu.edu.cn*
// Equally contributed.

† Electronic Supplementary Information (ESI) available: Synthesis procedure and spectral data. See DOI: 10.1039/x0xx00000x

View Article Online
DOI: 10.1039/C7NJ04212D

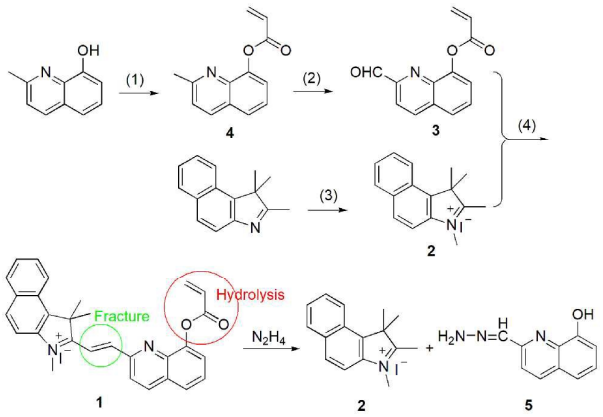

Scheme 1 Synthetic route of probe **1** and its recognition mechanism toward hydrazine. (1) Acryloyl chloride, CH_2Cl_2, Et_3N, rt, 12 h; (2) SeO_2, 1,4-dioxane, 101°C, rf, 4 h; (3) CH_3I, acetonitrile, reflux, 12 h; (4) ethanol, reflux, 12 h.

Experimental section

Methods and materials

8-hydroxy-2-methylquinoline, acryloyl chloride, CH_2Cl_2, Et_3N, SeO_2, 1,4-dioxane, CH_3I, acetonitrile, ethanol, NaCl, $MgCl_2$, KCl, $CaCl_2$, $MnCl_2$, $Co(NO_3)_2$, $Ni(NO_3)_2$, $ZnCl_2$, $Cd(NO_3)_2$, NaF, NaBr, NaI, $NaNO_3$, $NaClO_4$, Na_2SO_4, Na_2HPO_4, $NaClO_3$, $Na_2S_2O_3$, $Na_2C_2O_4$, Na_2SO_3, CH_3COONa, NaHS, Na_2N_3 Ile, Val, Ser, Gly, Trp, Thr, Phe, Cys, Met, Pro, Leu, Ala, Gln, Tyr, His, Hcy, Glu, and H_2O_2. All commercial grade chemicals and solvents were purchased and were used without further purification.

Mass spectra were obtained on high resolution mass spectrometer (IonSpec4.7 Tesla FTMS-MALDI/DHB). ^1H and ^{13}C NMR spectra were recorded on a Bruker 400 NMR spectrometer. Chemical shifts were reported in parts per million using tetramethylsilane (TMS) as the internal standard.

All spectral characterizations were carried out in HPLC-grade solvents at 20°C within a 10 mm quartz cell. UV-vis absorption spectra were measured with a TU-1901 double-beam UV-vis spectrophotometer. Fluorescence spectroscopy was determined on a Hitachi F-4600 spectrometer.

Synthesis of Compound 2

1,1,2-trimethylbenzo[e]indolenine (1.0452 g, 5 mmol) and CH_3I (1 mL) were dissolved in 15 mL acetonitrile, and the mixture was heated to 45℃. After 13 hours of reaction, the mixture was cooled to room temperature and a large amount of diethyl ether was poured into the reaction solution. The final product was obtained after filtration (0.9234 g, yield: 52.6%).

Characterization of **2**: ^1H NMR δ_H (DMSO, 400 MHz): 8.38 (d, 1H), 8.31 (d, 1H), 8.22 (d, 1H), 8.12 (d, 1H), 7.78 (t, 1H), 7.76(t, 1H), 4.10 (s, 3H), 2.88 (s, 3H), 1.76 (s, 6H). ^{13}C NMR: δ_C (100 MHz, DMSO): 196.37, 139.94, 136.97, 133.49, 130.98, 130.21, 128.84, 127.59, 127.58, 123.88, 113.62, 55.72, 35.59, 21.75, and 14.48.

Synthesis of compound probe 1

Compounds **2** (0.3513 g, 1.0 mmol) and **3** (0.2771 g, 1.0 mmol) were dissolved in 10 mL ethanol and the mixture was heated to 78℃. After refluxing for 12 h, the reaction mixture was cooled to room temperature. The final product probe **1** as brown solid was obtained after filtration (0.2528 g, 45.1%).

Characterization of **1**: HRMS (EI) m/z: calcd for $C_{29}H_{25}N_2O_2$ [M-I], 433.1911; found, 433.1839. ^1H NMR δ_H (DMSO, 400 MHz)：8.75(d, 1H), 8.66 (d, 1H), 8.51 (d,1H), 8.35 (t, 3H), 8.28 (d, 1H), 8.22 (d, 1H), 8.14 (d, 1H), 8.05 (m, 1H), 7.86 (t, 1H),7.79 (m, 3H), 6.78 (d, 2H), 6.36 (t, 1H), 4.25 (s, 3H), and 2.05 (s, 6H). ^{13}C NMR: δ_C (100 MHz, DMSO): 182.49, 164.86, 152.03, 148.53, 147.75, 139.95, 138.48,134.68, 133.98, 131.61, 130.53, 130.20, 129.09, 128.69, 130.20,128.12, 127.11, 126.63, 125.29, 123.98, 123.06, 117.15, 114.02, 54.71, 36.01, 25.08.

Cell incubation and imaging

Cell viability, as a testing endpoint of cytotoxicity, was determined with 3-(4,5-dimethylthiazol-2-yl)-2,5-diphenyltetrazolium bromide (MTT) assay. $HepG_2$ cells were seeded into 96-well plates at a density of 5×10^3 cells per well in DMEM (10% FBS) in six replicates and incubated for 24 h. After that the cells were exposed to 2, 4, 6, 8, 10 μM probe **1** for 1 h, then medium was discard and replaced with 100 μL fresh medium for 24 h, then 20 μL MTT (5 mg/mL) was added, and the cells were further incubated for 4 h at 37°C. The medium was removed and the formazan crystals were dissolved in DMSO. The optical density (OD) was measured at 490 nm.

The intrinsic ability of probe **1** to target mitochondrion was investigated in living $HepG_2$ cells. The cells were stained with probe **1** (1.0×10^{-5} M, 30 min, 37°C) and washed twice with PBS, then co-stained further with a commercially available mito tracker (100 nM, 30 min) in the culture medium. After removing the culture medium and washed twice with PBS, The imaging results were obtained, which show that the green image for the 1 channel was obtained upon excitation at 488 nm and the red image for the 2 channel was obtained upon excitation at 495 nm.

The $HepG_2$ cells were incubated with probe **1** for ratio imaging. The fluorescent images were recorded at green and red channels with 525±50 nm and 595±50 nm filters separately, and the ratio images were got with the intensity ratio of the green/red after the cells incubated with probe **1** (1.0×10^{-5} M, 37°C) for 30 min. After adding 1×10^{-3} M hydrazine hydrate and incubation for 30 min, the fluorescent and ratio images were taken at the same situation. The excitation was performed at 405 nm.

Results and discussion

Sensing of the probe 1 to hydrazine

To study the recognition properties of probe **1** toward hydrazine, UV-vis and fluorescence titration experiments (Figures **S1** and **S2** in Supporting Information and **Fig. 1**) were conducted with 0.1 M hydrazine in aqueous solution of probe **1** [3.0×10^{-5} M in 100:1 (v/v) water/DMSO]. Upon addition of

DOI: 10.1039/C7NJ04212D

hydrazine, the peaks at 375 and 430 nm in the UV-vis spectrum decreased gradually while a new band developed at 240 nm, and then, the band reached the highest intensity at 6.0 equiv of Hydrazine (**Fig. S1** in Supporting Information). Meanwhile, one clear isosbestic point was observed at 331 nm, indicating that only one product was generated from the reaction of 1 with hydrazine (**Fig. S1** in Supporting Information). The solution color changed by degrees from yellow to colorless in the presence of different concentrations of hydrazine (**Fig. S2** in Supporting Information). As shown in **Fig. 1a**, upon excitation at 405 nm, one emission band centered at 590 nm appeared in the fluorescence spectrum of probe **1** [3.0×10^{-5} M in 100:1 (v/v) water/DMSO]. Upon gradual addition of hydrazine, the emission at 590 nm decreased while a new peak at 467 nm increased with no change of the emission intensity at 520 nm observed (**Fig 1a**). As demonstrated in **Fig. 1b**, in the concentration range of 30 to 180 μM, the ratio of I_{590}/I_{520} was in good linear relationship with hydrazine concentration, implying that hydrazine can be quantitatively detected in a wide concentration range in a ratiometric fluorescence mode. From the linear calibration graph with the fluorescence titration experiment (**Fig. 1b**), the detection limit of probe **1** for hydrazine was figured out to be about 2.1 μM based on signal-to-noise ratio (S/N) = 3,[48,49] Further experiments indicated that the fluorescence color of probe **1** aqueous solution changed from orange red to colorless under 365 nm light excitation (**Fig. 1c**). These results led us to conclude that probe **1** could be an effective ratiometric fluorescent probe for hydrazine.

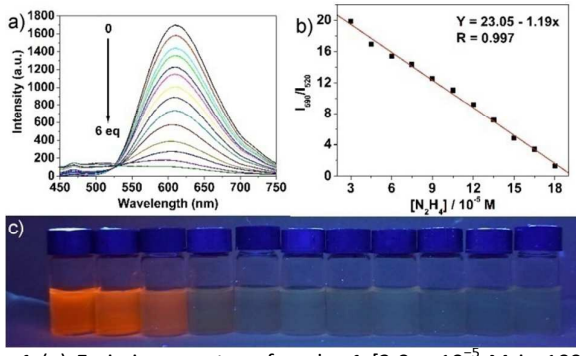

Fig. 1 (a) Emission spectra of probe **1** [3.0×10^{-5} M in 100:1 (v/v) water/DMSO] upon titration of hydrazine (0–6.0 equiv to **1**) with excitation at 405 nm. (b) The linearity of emission intensity ratio of I_{590}/I_{520} with hydrazine concentration increase. (c) Photographs of probe **1** [3.0×10^{-5} M in 100:1 (v/v) water/DMSO] upon addition of hydrazine at various concentrations (0 M, 3.0×10^{-5} M, 6.0×10^{-5} M, 1.2×10^{-4} M, 1.5×10^{-4} M, 1.8×10^{-4} M, from left to right) in water and under a UV lamp (365 nm). The reaction time was 4 min.

Mechanism studies

The recognition mechanism was studied by Mass spectrometry. For pure probe **1**, a characteristic peak at m/z = 433.1839 was obtained which corresponds to the species **1** [M-I], whilst after reaction with hydrazine, the peak at 433.1839 disappeared and two new peaks appeared at m/z = 224.1441 and 188.0802, which are corresponding to compounds **2** (M-I) and **5** (M+1), indicating the decomposition of probe **1** and the formation of compounds **2** and **5** (**Scheme 1**).

In order to further study its recognition mechanism, using the reaction of compound **3** and hydrazine, compound **5** was obtained, which was characterized with ^{1}H NMR (**Fig. S3** in Supporting Information). In addition, the emission spectra of compounds **2** and **5** were also tested (**Fig. S4** in Supporting Information), which are in accordance with the emission spectral change of probe **1** upon addition of hydrazine (**Fig. 1a**).

pH range in application of probe 1 toward hydrazine

The pH value of solution was found to be essential to the reaction between probe **1** and hydrazine. To investigate the pH effect, the fluorescence of 3.0×10^{-5} M probe **1** in the absence and presence of 1.8×10^{-4} M hydrazine were examined at pH range from 0 to 14.0. As shown in **Fig. S5**, probe **1** itself is stable and its emission spectra hardly changed in a wide pH range from 1.0 to 10.0. However, upon addition of hydrazine, there was a significant fluorescence change in pH range of 5.0–10.0. Notably, the fluorescence changes of probe **1** to hydrazine reached a maximum at about 5.0 and became almost constant in the pH range of 5.0–10.0. Such result implies that probe **1** is able to detect hydrazine in a relatively wide pH range.

Selectivity and competition studies

To evaluate the selectivity of probe **1** for hydrazine, various species including nucleophilic molecules (DIPEA, Phenol, Thiourea, TEA, and Urea), metal ions (Na^+, Mg^{2+}, K^+, Ca^{2+}, Mn^{2+}, Co^{2+}, Ni^{2+}, Zn^{2+}, and Cd^{2+}), anions (F^-, Cl^-, Br^-, I^-, NO_3^-, ClO_4^-, SO_4^{2-}, $H_2PO_4^-$, ClO_3^-, $S_2O_3^{2-}$, $C_2O_4^{2-}$, SO_3^{2-}, HS^-, CH_3COO^-, and N_3^-) and biological species (Ile, Val, Ser, Gly, Trp, Thr, Phe, Cys, Met, Pro, Leu, Ala, Gln, Tyr, His, Hcy, Glu, and H_2O_2) were tested. As shown in figures **S6**, **S7**, **S8**, **S9**, red bars of figures **S10**, **S11**, **S12** in Supporting Information and **Fig. 2**, only hydrazine induced a significant fluorescence quenching, whilst, other tested species did not induce any obvious fluorescence quenching. Some reported probes containing C=C can detect some anions such as $ONOO^-$, ClO^-, SO_3^{2-},[50-52] while $ONOO^-$ and SO_3^{2-} have no such influence on our probe, indicating the high selectivity toward hydrazine. Addition of ClO^- can make the emission change in both the peak and intensity of probe **1** (**Fig. S9**), which needs us to study further in our future work.

To further assess its utility as a hydrazine-selective fluorescent probe, its fluorescent response to hydrazine in complicated surroundings as mentioned above was also tested (green bars of figures **S10**, **S11**, **S12** in Supporting Information and **Fig. 2**). The results evidenced that all of the selected species have no interference in the detection of hydrazine. This result strongly indicated that probe **1** could be an excellent fluorescent probe towards hydrazine with strong anti-interference ability.

View Article Online
DOI: 10.1039/C7NJ04212D

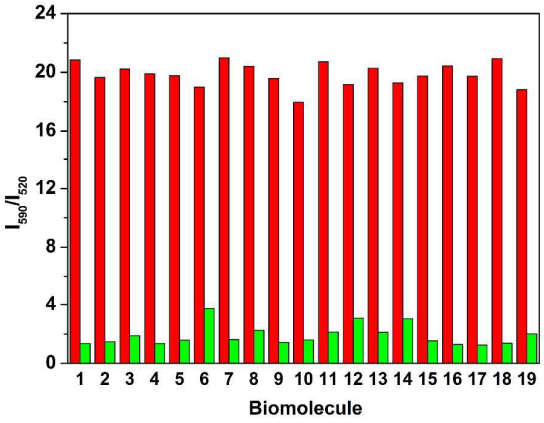

Fig. 2 Fluorescence responses of **1** [3.0 × 10^{-5} M in 100:1 (v/v) water/DMSO] upon addition of different species (6 equiv of species relative to **1**) (red bars) and fluorescence changes of the mixture of **1** and hydrazine (1.8 × 10^{-4} M in water) after addition of an excess of the indicated species (6 equiv relative to **1**) (green bars). The excitation wavelength was 405 nm. I_{590} and I_{520} represent the emission intensity at 590 and 520 nm. The reaction time was 4 min. The biomolecules used were Ile, Val, Ser, Gly, Trp, Thr, Phe, Cys, Met, Pro, Leu, Ala, Gln, Tyr, His, Hcy, Glu, and H_2O_2.

An ideal probe ought to have good photostability and thermal stability. As shown in **Fig. 3a**, the emission intensity ratio of probe **1** [3.0 × 10^{-5} M in 100:1 (v/v) water/DMSO] at 590 and 520 nm (I_{590}/I_{520}) hardly changes with irradiation time extending, indicating excellent photostability. When the temperature increased from 30 to 42°C, the emission intensity ratio I_{590}/I_{520} doesn't change (**Fig. 3b**). Such results suggest that probe **1** as a hydrazine probe possesses excellent photostability and thermal stability.

hydrazine in time-dependent fluorescence spectra of probe **1**probe **1**hydrazine is completely accomplished within 4 min and hydrazine can be detected within 2 min when the concentration of hydrazine is higher or equal to 1.8 × 10^{-4} M. Such result further proved the fast response and high sensitivity of probe **1** for detection of hydrazine.

The cytotoxicity of probe **1** toward $HepG_2$ cells was measured using the 3-(4,5-dimethylthiazol-2-yl)-2,5-diphenyltetrazilium bromide (MTT) assay to evaluate the potential application of probe **1** in live cell imagining. The cellular viability was estimated to be greater than 86% after 1 h at the concentration of 10^{-5} M for probe **1**, suggesting the low cytotoxicity of probe **1** (**Fig. 3d**).

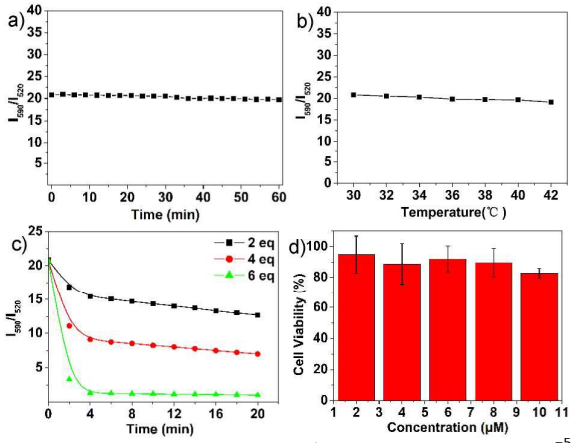

Fig. 3 Emission intensity ratio I_{590}/I_{520} of probe **1** [3.0 × 10^{-5} M in 100:1 (v/v) water/DMSO] with irradiation (λ_{ex} = 405 nm) time (a) and temperature (b) change. Kinetic curve of probe **1** [3.0 × 10^{-5} M in 100:1 (v/v) water/DMSO] at 590 nm and 520 nm with hydrazine at different concentrations (the concentrations of hydrazine are 6.0 × 10^{-5} M (black line), 1.2 × 10^{-4} M (red line), and 1.8 × 10^{-4} M (green line). The excitation wavelength was 405 nm (c). Viability assay for $HepG_2$ cells treated with probe **1** in dark (d).

Application of the probe 1 in living cells

The intrinsic ability of probe **1** to target mitochondrion was investigated in living $HepG_2$ cells. The cells stained with probe **1** (1.0 × 10^{-5} M 30 min, 37°C) were co-stained further with the commercially available mitochondrion-Tracker (100 nM, 30 min) in the culture medium. The imaging results show that the red image for **1** channel obtained upon excitation at 595 nm is almost identical to the green image for the mitochondrion-Tracker channel obtained upon excitation at 488 nm (**Fig. 4**), suggesting the ability of probe **1** to target mitochondrion. The targeting ability of this probe toward mitochondrion may be ascribed to the cationic cyanine moiety.

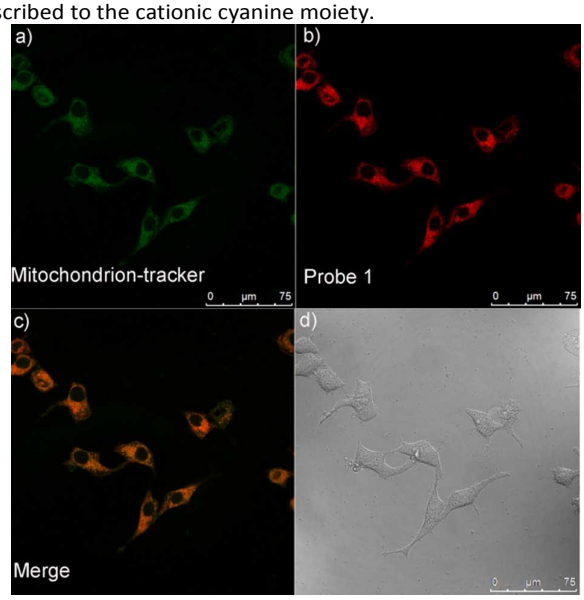

Fig. 4 Confocal fluorescence images of $HepG_2$ cells stained with mitochondrion-Tracker for 30 min (a) and **1** (1.0 × 10^{-5} M) for 30 min (b). (c) Merged image of (a) and (b). (d) Bright-field image.

View Article Online
DOI: 10.1039/C7NJ04212D

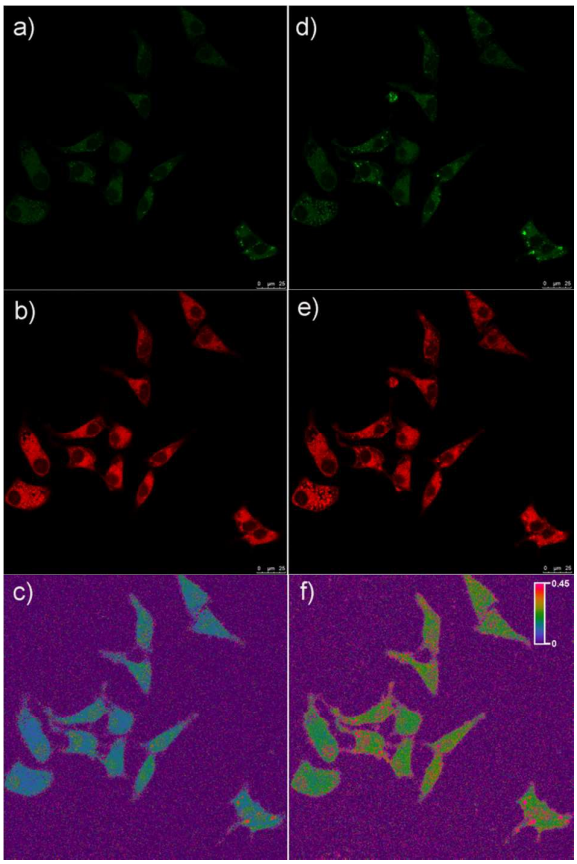

Fig. 5 Ratiometric confocal fluorescence images in live $HepG_2$ cells constained by 10^{-5} M probe **1** (a–c) and cells of pretreated with 10^{-4} M probe **1** followed by incubation with 10^{-3} M hydrazine for 30 min (d–f). Emission was collected by green channel at 525 ± 50 nm (a and d) and red channel at 595 ± 50 nm (b and d), under excitation at 405 nm. (c and f) Ratiometric confocal fluorescence images with ratio of red to green channels.

Practical applications of probe **1** in imaging live $HepG_2$ cells were investigated using confocal fluorescence microscopy with a 405 nm diode laser. The confocal fluorescence microscopy images are shown in **Fig. 5**. After incubation of $HepG_2$ cells with probe **1** (1.0×10^{-5} M) for 30 min at 37°C, weak fluorescence was detected at green (525±25 nm) and strong fluorescence at red (595±25 nm) channels in the cytoplasm, demonstrating the good cell permeability of probe **1**. Following addition of hydrazine (1.0×10^{-3} M), although no obvious change was observed at the green and red channels, a rapid and obvious change at the ratiometric confocal fluorescence was observed (figures **5c** and **5f**), suggesting the reaction of probe **1** to hydrazine. The emission ratio at the green channel to the red channel increased from 0.2003 to 0.2396, indicating the advantage of the ratiometric fluorescence imaging. Bright-field measurements indicated that the cells before and after treatment with hydrazine remained viable throughout the imaging experiments (**Fig. S13** in Supporting Information).

Conclusions

In summary, a ratiometric fluorescent hydrazine-probe was synthesized and demonstrated. This probe can not only quantitatively detect hydrazine in wide concentration range, exhibits excellent selectivity, anti-interference, fast response time, good location ability toward mitochondrion and the ability of selective detection of hydrazine in living cells.

Acknowledgements

We are grateful for the financial supports from National Natural Science Foundation of China (U1704161, U1504203, 21601158, 21571133, and 21171120), Zhengzhou University (32210431), Beijing Natural Science Foundation Program and Scientific Research Key Program of Beijing Municipal Commission of Education (KZ201710025024), and Natural Science Foundation of Beijing Municipality (7132020).

Notes and references

1 A. D. Sutton, A. K. Burrell, D. A. Dixon, E. B. Garner, J. C. Gordon, T. Nakagawa, K. C. Ott, P. Robinson and M. Vasiliu, *Science*, 2011, **331**, 1426.
2 J. Sanabria-Chinchilla, K. Asazawa, T. Sakamoto, K. Yamada, H. Tanaka and P. Strasser, *J. Am. Chem. Soc.*, 2011, **133**, 5425.
3 T. Sakamoto, K. Asazawa, J. Sanabria-Chinchilla, U. Martinez, B. Halevi, P. Atanassov, P. Strasser and H. Tanaka, *J. Power Sources*, 2014, **247**, 605.
4 A. Serov, M. Padilla, A. J. Roy, P. Atanassov, T. Sakamoto, K. Asazawa and H. Tanaka, *Angew Chem. Int. Ed.,* 2014, **53**, 10336.
5 R. Ahmad, N. Tripathy, D. U. J. Jung and Y. B. Hahn, *Chem. Commun.*, 2014, **50**, 1890.
6 S. D. Zelnick, D. R. Mattie and P. C. Stepaniak, *Aviat. Space Envir. Md.*, 2003, **74**, 1285.
7 T. Tang, Y. Q. Chen, B. S. Fu, Z. Y. He, H. Xiao, F. Wu, J. Q. Wang, S. R. Wang and X. Zhou, *Chin. Chem. Lett.*, 2016, **27**, 540.
8 Y. Qian, J. Lin, LJ. Han, L. Lin, and H. L. Zhu, *Biosens. Bioelectron*, 2014, **58**, 282.
9 A. Umar, M. M. Rahman, S. H. Kim, and Y. B. Hahn, *Chem. Commun.*, 2008, 166.
10 E. Gionfriddo, A. Naccarato, G. Sindona and A. Tagarelli, *Anal. Chim. Acta*, 2014, **835**, 37.
11 J-A. Oh, J-H. Park and H-S. Shin, *Anal. Chim. Acta*, 2013, **769**, 79.
12 L. Cui, K. Jiang, D. Q. Liu and K. L. Facchine, *J. Chromatogr A*, 2016, **1462**, 73.
13 D. S. Kosyakov, A. S. Amosov, N. V. Ul'yanovskii, A. V. Ladesov, Y. G. Khabarov and O. A. Shpigun, *J. Anal. Chem.*, 2017, **72**, 171.
14 G. Dutta, S. Nagarajan, LJ. Lapidus and P. B. Lillehoj, *Biosens. Bioelectron.*, 2017, **92**, 372.
15 R. Gupta, P. K. Rastogi, V. Ganesan, D. K. Yadav and P. K. Sonkar, *Sens. Actuators B*, 2017, **239**, 970.
16 F. A. Harraz, A. A. Ismail, S. A. Al-Sayari, A. Al-Hajry and M. S. Al-Assiri, *Sens. Actuators B*, 2016, **234**, 573.
17 J. Wu, T. Zhou, Q. Wang and A. Umar, *Sens. Actuators B*, 2016, **224**, 878.
18 B. Fang, C. H. Zhang, W. Zhang and G. F. Wang, *Electrochim. Acta*, 2009, **55**, 178.
19 H. Zhang, R. Liu, J. Liu, L. Li, P. Wang, S. Q. Yao, Z. Xu and H. Sun, *Chem. Sci.*, 2016, **7**, 256.
20 H. Chen, Y. Tang, M. Ren and W. Lin, *Chem. Sci.*, 2016, **7**, 1896.

View Article Online
DOI: 10.1039/C7NJ04212D

21 Y. Tang, X. Kong, A. Xu, B. Dong and W. Lin, *Angew Chem. Int. Ed.*, 2016, **55**, 3356.
22 W. Xu, Z. Zeng, J-H. Jiang, Y-T. Chang and L. Yuan, *Angew Chem. Int. Ed.*, 2016, **55**, 13658.
23 R. Zhang, J. Zhao, G. Han, Z. Liu, C. Liu, C. Zhang, B. Liu, C. Jiang, R. Liu, T. Zhao, M-Y. Han and Z. Zhang, *J. Am. Chem. Soc.*, 2016, **138**, 3769.
24 W. Chen, A. Pacheco, Y. Takano, J. J. Day, K. Hanaoka and M. Xian, *Angew Chem. Int. Ed.*, 2016, **55**, 9993.
25 W. Zhou, Y. Cao, D. Sui and C. Lu, *Angew Chem. Int. Ed.*, 2016, **55**, 4236.
26 A. K. Steiger, S. Pardue, C. G. Kevil and M. D. Pluth, *J Am. Chem. Soc.*, 2016, **138**, 7256.
27 X. Wu, L. Li, W. Shi, Q. Gong and H. Ma, *Angew Chem. Int. Ed.*, 2016, **55**, 14728.
28 T. Pinkert, D. Furkert, T. Korte, A. Herrmann and C. Arenz, *Angew Chem. Int. Ed.*, 2017, **56**, 2790.
29 W. Shao, G. Chen, A. Kuzmin, H. L. Kutscher, A. Pliss, T. Y. Ohulchanskyy and P. N. Prasad, *J. Am. Chem. Soc.*, 2016, **138**, 16192.
30 M. H. Lee, B. Yoon, J. S. Kim and J. L. Sessler, *Chem. Sci.*, 2013, **4**, 4121.
31 L. Cui, Z. Peng, C. Ji, J. Huang, D. Huang, J. Ma, S. Zhang, X. Qian and Y. Xu, *Chem. Commun.*, 2014, **50**, 1485.
32 D. Y. Zhou, Y. Y. Wang, J. Jia, W. Z. Yu, B. F. Qu, X. Li and X. Sun, *Chem. Commun.*, 2015, **51**, 10656.
33 M. Sun, J. Guo, Q. Yang, N. Xiao and Y. Li, *J. Mater. Chem. B*, 2014, **2**, 1846.
34 K. Vijay, C. Nandi and S. D. Samant, *RSC Adv.*, 2014, **4**, 30712.
35 S. I. Reja, N. Gupta, V. Bhalla, D. Kaur, S. Arora and M. Kumar, *Sens. Actuators B*, 2016, **222**, 923.
36 M. G. Choi, J. O. Moon, J. Bae, J.W. Lee and S-K. Chang, *Org Biomol. Chem.*, 2013, **11**, 2961.
37 J. S. Wu, B. Kwon, W. M. Liu, E. V. Anslyn, P. F. Wang, and J. S. Kim, *Chem Rev.*, 2015, **115**, 7893.
38 Z. Li, X. Liu, W. Zhao, S. Wang, W. Zhou, L. Wei and M. Yu, *Anal. Chem.*, 2014, **86**, 2521.
39 M. Lan, Wu J, W. Liu, W. Zhang, J. Ge, H. Zhang, J. Sun, W. Zhao and P. Wang, *J. Am. Chem. Soc.*, 2012, **134**, 6685.
40 J. Fan, M. Hu, P. Zhan and X. Peng, *Chem. Soc. Rev.*, 2013, **42**, 29.
41 J. Fan, W. Sun, M. Hu, J. Cao, G. Cheng, H. Dong, K. Song, Y. Liu, S. Sun and X. Peng, *Chem. Commun.*, 2012, **48**, 8117.
42 C. Hu, W. Sun, J. Cao, P. Gao, J. Wang, J. Fan, F. Song, S. Sun and X. Peng, *Org. Lett.*, 2013, **15**, 4022.
43 S. Goswami, S. Paul and A. Manna, *New J. Chem.*, 2015, **39**, 2300.
44 S. Goswami, K. Aich, S. Das, S. B. Roy, B. Pakhira and S. Sarkar, *RSC Adv.*, 2014, **4**, 14210.
45 S. Goswami, S. Paul and A. Manna, *RSC Adv.*, 2013, **3**, 18872.
46 S. Goswami, S. Das, K. Aich, D. Sarkar and T. K. Mondal *Tetrahedron Lett.*, 2014, **55**, 2695.
47 S. Goswami, S. Das, K. Aich, B. Pakhira, S. Panja, S. K. Mukherjee and S. Sarkart, *Org. Lett.*, 2013, **15**, 5412.
48 D. Oushiki, H. Kojima, T. Terai, M. Arita, K. Hanaoka, Y. Urano and T. Nagano, *J. Am. Chem. Soc.*, 2010, **132**, 2795.
49 C. Zhao, X. Zhang, K. Li, S. Zhu, Z. Guo, L. Zhang, F. Wang, Q. Fei, S. Luo, P. Shi, H. Tian and W-H. Zhu, *J. Am. Chem. Soc.*, 2015, **137**, 8490.
50 Z. Zhang, J. Fan, G. Cheng, S. Ghazali and J. Du, X. Peng, *Sens. Actuat. B-Chem.*, 2017, **246**, 293.
51 D. Cheng, Y. Pan, L. Wang, Z. Zeng, L. Yuan, X. Zhang and Y-T. Chang, *J. Am. Chem. Soc.*, 2017, **139**, 285.
52 Y. Wu, J. Wang, F. Zeng, S. Huang, J. Huang, H. Xie, C. Yu and S. Wu, *ACS Appl. Mater. Interfaces*, 2016, **8**, 1511.

View Article Online
DOI: 10.1039/C7NJ04212D

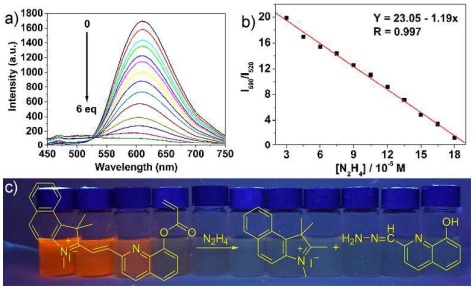

A fluorescent hydrazine-probe was synthesized, which exhibited high sensitivity, excellent selectivity and anti-interference ability.